ARTICLE

BIOTECHNOLOGY and BIOENGINEERING

Expansion of Mouse Embryonic Stem Cells on Microcarriers

Elsa Abranches,[1] Evguenia Bekman,[2] Domingos Henrique,[2] Joaquim M.S. Cabral[1]

[1]Centro de Engenharia Biológica e Química, Instituto Superior Técnico, Av. Rovisco Pais, 1049-001 Lisboa, Portugal; telephone: +351 218 419 065; fax:+351 218 419 062; e-mail: joaquim.cabral@ist.utl.pt

[2]Instituto de Medicina Molecular, Faculdade de Medicina de Lisboa, Av. Professor Egas Moniz, Lisboa, Portugal

Received 22 April 2006; accepted 22 August 2006

Published online 27 September 2006 in Wiley InterScience (www.interscience.wiley.com). DOI 10.1002/bit.21191

ABSTRACT: Embryonic stem (ES) cells have been shown to differentiate in vitro into a wide variety of cell types having significant potential for tissue regeneration. Therefore, the operational conditions for the ex vivo expansion and differentiation should be optimized for large-scale cultures. The expansion of mouse ES cells has been evaluated in static culture. However, in this system, culture parameters are difficult to monitor and scaling-up becomes time consuming. The use of stirred bioreactors facilitates the expansion of cells under controlled conditions but, for anchorage-dependent cells, a proper support is necessary. Cytodex-3, a microporous microcarrier made up of a dextran matrix with a collagen layer at the surface, was tested for its ability to support the expansion of the mouse S25 ES cell line in spinner flasks. The effect of inocula and microcarrier concentration on cell growth and metabolism were analyzed. Typically, after seeding, the cells exhibited a growth curve consisting of a short death or lag phase followed by an exponential phase leading to the maximum cell density of $2.5–3.9 \times 10^6$ cells/mL. Improved expansion was achieved using an inoculum of 5×10^4 cells/mL and a microcarrier concentration of 0.5 mg/mL. Medium replacement allowed the supply of the nutrients and the removal of waste products inhibiting cell growth, leading to the maintenance of the cultures in steady state for several days. These conditions favored the preservation of the S25 cells pluripotent state, as assessed by quantitative real-time PCR and immunostaining analysis.

Biotechnol. Bioeng. 2007;96: 1211–1221.

KEYWORDS: embryonic stem cells; expansion; spinner flasks; cytodex-3; scale-up

Introduction

Mouse embryonic stem (ES) cells are pluripotent cells isolated from the inner cell mass of the blastocyst. They can be expanded in vitro and have the ability to give rise to cells from the three germ layers (Smith, 2001). Since their isolation in the early 1980s (Evans and Kaufman, 1981; Martin, 1981), ES cells have been shown to differentiate into a wide variety of cell types (Keller, 1995; Rathjen et al., 2002), including all three neuronal lineages (Bain et al., 1995; Fraichard et al., 1995).

These properties make them promising tools for drug screening, tissue engineering, and cellular therapies, including the treatment of several disorders, such as neurodegenerative diseases. To make use of the vast potential of ES cells, a better understanding of factors influencing their proliferation and differentiation is required for the efficient in vitro cell expansion. In general, the long-term and/or large-scale expansion of ES cells in vitro is feasible but requires optimized culture conditions. Numerous reports have been published using ES cells as a model to study expansion and differentiation conditions but few of them address their scaling-up to large cell numbers (Fok and Zandstra, 2005; Fong et al., 2004; Oh et al., 2005).

In our previous studies, the expansion of ES cells has been evaluated in static culture (Abranches et al., 2003, 2006, manuscript under revision). However, in this system, culture parameters are difficult to monitor and scaling-up becomes time consuming.

The use of stirred bioreactors facilitates the expansion of cells under controlled conditions while providing a homogeneous environment. However, for anchorage-dependent cells, a proper support is necessary. A simple method of scaling-up for adherent cells makes use of microcarriers.

Correspondence to: J.M.S. Cabral

Contract grant sponsor: Fundação para a Ciência e a Tecnologia, Portugal
Contract grant number: POCTI/BIO/46695/2002

Since the development of microcarriers by van Wezel (1967), different materials and surface types have been employed as supports for the cell growth (Reuveny, 1990). This strategy takes advantage of the increased available surface area provided by these supports. As a result, this system allows high cell density per unit volume due to the high surface area to volume ratio, as well as an efficient control and monitoring of different environmental parameters, together with easy cell sampling and harvesting (Reuveny, 1990).

Cytodex-3 (GE Healthcare), a microporous microcarrier made up of a dextran matrix with a collagen layer at the surface, has been successfully used for the expansion of primary cells as well as established cell lines (Amersham-Biosciences; Fok and Zandstra, 2005; Santos et al., 2005). One gram of dry weight of this support has approximately 3.0×10^6 microcarriers and an approximate surface area of 2,700 cm^2. Its ability to support the growth of the mouse S25 ES cell line in spinner flasks was tested in this study.

The study of the S25 cell line is important for experimental analysis of different aspects of mammalian neural development as well as a possible source for transplantation-based cell therapy. This mouse ES cell line was derived from the E14TG2a cell line (Billon et al., 2002; Li et al., 1998). It has the selection/marker cassette β-geo introduced into the *Sox2* allele, which is a gene expressed both in undifferentiated ES cells and in the developing neuroepithelium. Therefore, this cassette (in-frame fusion between β-galactosidase and neomycin phosphotransferase coding sequences) allows lineage selection of cells expressing *Sox2*. This mouse ES cell line was shown to have similar efficiency of neural commitment and terminal neuronal differentiation as compared to the parental E14TG2a and another E14TG2a-derived line, 46C (Bekman and Henrique, unpublished data). The proliferation rate of this cell line in self-renewal conditions also compares well to other feeder-independent mouse ES cell lines (Fok and Zandstra, 2005; Oh et al., 2005; Viswanathan et al., 2003). For these reasons, the results obtained in this study may be fully applicable to other feeder-independent mouse ES cell lines.

A number of parameters may influence cell culture, thus, several factors were analyzed in order to establish more favorable conditions for this cell line expansion, namely the inocula and the microcarrier concentration.

The S25 ES cell line, due to its characteristics, can be easily and efficiently induced into neural differentiation. The ability of these cells to give rise to neural phenotypes after expansion in spinner flasks was also assessed.

Materials and Methods

Cell Culture

Mouse ES cells (S25, E14TG2a-derived cell line) (Billon et al., 2002; Li et al., 1998) were a gift from Meng Li and Austin Smith (Institute for Stem Cell Research, Edinburgh University, Scotland, UK).

In control experiments (static cultures), cell culture was performed as described in Li et al. (1998) and Abranches et al. (2003). Briefly, ES cells were grown at 37°C in a 5% (v/v) CO_2 incubator in Glasgow Modified Eagles Medium (GMEM, Biological Industries, Beit Haemek, Israel), supplemented with 10% (v/v) fetal bovine serum (Gibco, Burlington, Ontario, Canada), 1 mM 2-mercaptoethanol, 1× non-essential amino acids, 1 mM sodium pyruvate, and 2 mM glutamine. Leukemia inhibitory factor (LIF) produced in-house was added at 5 ng/mL for the expansion in adherent conditions.

For spinner experiments, protocols were adapted based on the recommendations for microcarrier cultures using Cytodex-3 (GE Healthcare, Berkshire, UK). All experiments were performed in duplicate, save otherwise noted, and data are expressed as the means of the two independent experiments ± standard deviation (SD).

Experiments were normalized for the same concentration in terms of cells per mL, as this would enable a better comparison between the two different optimized parameters (inoculum and microcarrier concentration). Nevertheless, S25 cells are anchorage-dependent cells and consequently, their growth depends on the available surface area (Table I). Therefore, the comparison of initial and final data was also performed using concentrations in terms of cells per cm^2 (Table II).

Controls

Cells were seeded on 24-well gelatin-coated plates at the same concentration, in terms of cells per mL, as for the microcarriers, and medium was changed at the same frequency as for the spinner flasks experiments.

Spinner Flasks

For stirred microcarrier cultures, 100-mL spinner flasks from *Bellco Biotechnology* (Bellco Glass, Inc., Vineland, NJ; model #1965) were used, with a final media volume of 80 mL and a stirring speed of 40 rpm. Spinner flasks were siliconized before use with sigmacote (Sigma, St. Louis, MO).

Required quantities of Cytodex-3 were weighted (final concentrations of 0.5 and 3.0 mg/mL), hydrated,

Table I. Available surface areas for the tested conditions, for the stirred microcarrier cultures, and the control plates.

Culture type	Cytodex-3 concentration		Media volume (mL)	Total available area (cm^2)
	mg/mL	cm^2/mL		
Stirred microcarrier cultures	0.5	1.35	80	108
	3.0	8.10	80	648
Control plates	—	3.80	0.50	1.9

DOI 10.1002/bit

Table II. Initial and final cell densities, and fold increase of S25 cells grown in stirred microcarrier cultures and control plates.

	Initial cell density			Final cell density		
Culture type	10^6 cells/mL	10^6 cells/cm^2	Cells/bead	10^6 cells/mL	10^6 cells/cm^2	Fold Increase
Stirred microcarrier cultures	0.010	0.0012	1	2.5 ± 2.0	0.31 ± 0.25	249 ± 199
	0.050	0.0062	6	3.4 ± 1.2	0.42 ± 0.15	67 ± 24
		0.037*	33*	4.0 ± 0.72*	3.0 ± 0.54*	80 ± 14*
	0.100	0.012	11	3.9 ± 0.91	0.48 ± 0.11	39 ± 9.0
Control plates	0.010	0.0052	—	0.98 ± 0.07	0.51 ± 0.037	99 ± 7.0
	0.050	0.026	—	1.54 ± 0.25	0.81 ± 0.13	31 ± 5.0
	0.100	0.054	—	1.14 ± 0.59	0.60 ± 0.31	11 ± 3.0

For stirred cultures, 3 mg of Cytodex-3 per mL were used for the different inocula. The values denoted with an asterisk were obtained when using 0.5 mg of Cytodex-3 per mL. All experiments were averages of two independent runs.

and sterilized by autoclaving as recommended by the manufacturers. Microcarriers were equilibrated in culture medium for at least 30 min prior to cell addition in order to maximize cell attachment.

Cells were inoculated with the microcarriers in 50% of the final volume. Intermittent stirring (2 min every 30 min) was performed for 3 h. After this period, the volume was increased to 75% and intermittent stirring was performed for another 3 h. Finally, the volume was completed and constant stirring at 40 rpm was initiated.

Media changes (50%) were performed every day starting on day 2. For this, microcarriers were allowed to settle for 10 min, 50% of the supernatant was discarded, and new medium was added.

Sampling

Spinner flasks were removed from the incubator and placed in the laminar-flow hood on an agitated plate. Agitation was interrupted and samples were collected immediately in order to minimize variations due to the sedimentation of microcarriers.

Every day, 0.5-mL aliquots were collected for cell counting. Media samples were collected and stored for posterior analysis of glucose and lactate dehydrogenase (LDH). Microcarriers were washed twice with phosphate buffer saline (PBS). Trypsin (0.25%) (v/v) was added and cells were placed for 10 min in a 37°C water-bath. Occasional flicking was performed in order to facilitate detachment of cells from the beads. Medium was added to stop trypsinization and the supernatant with cells was collected into a new tube. Beads were washed twice to detach remaining cells and the supernatants were pooled. Cells were centrifuged and suspended in fresh medium. A sample was taken for counting and on days 4 and 8, the remaining cells were used for RNA extraction.

On days 4 and 8, 0.5–1.0 mL samples were also collected for cell staining.

On day 8, cells from 5-mL samples were also collected, counted, and plated on bacterial-grade petri dishes in order to assess cell differentiation potential through EB formation.

Embryoid Body Formation Assay and Neural Differentiation Potential

To assess the ability of S25 cells to form EBs after expansion in the stirred microcarrier system, cells were seeded on 60-mm bacterial-grade petri dishes at 1×10^5 cells/mL. Cells were plated in GMEM supplemented with 10% (v/v) fetal bovine serum (Gibco), in the absence of LIF, and medium was changed every other day. EBs formation was observed under an inverted microscope after 24–48 h.

For neural induction, 1 mM all *trans*-retinoic acid was added at days 4 and 6 of culture, and geneticin (G418) was added from day 6 onwards for positive selection of neural precursors. In order to assess the differentiation potential of the S25 ES cells under study, on day 8, EBs were dissociated and plated in conditions that promote neural differentiation (Li et al., 1998). Cultures were observed under an inverted microscope.

Cell Counts and Cell Viability

Cell density was determined using a hemacytometer and viability was determined using the standard Trypan Blue dye exclusion test. For each experiment, a sample was taken and cell counts were performed in duplicate.

Glucose and Lactate Dehydrogenase Analysis

Supernatant samples were collected throughout the experiments, centrifuged for 10 min at 1,500 rpm, and stored at −20°C for posterior analysis. Samples were processed as recommended by the kit's manufacturers before analysis.

Glucose levels were measured using the enzymatic kit from Boehringer Mannheim (Ingelheim, Germany), D-Glucose cat.no.0716251. The specific rate of glucose consumption was calculated for every time interval using the following equation: $q_{Gluc} = (\Delta\text{Glucose})/(\Delta t \times \Delta X_v)$, where ΔGlucose is the change in glucose concentration over the time period t, and ΔX_v is the logarithmic variation of viable cells during the same time period.

For determination of lactate dehydrogenase, an LDH analysis kit from Promega was used (CtoTox96 non-radioactive cytotoxicity assay, cat.no.G1782). The specific rate of LDH release was calculated for every time interval using the following equation: $q_{LDH} = (\Delta LDH)/(\Delta t \times \Delta X_v)$, where ΔLDH is the change in LDH concentration over the time period t, and ΔX_v is the logarithmic variation of viable cells during the same time period.

Quantitative RT-PCR Analysis

Total RNA was collected from cell samples on days 0, 4, and 8 using the High Pure RNA Isolation Kit (Roche, Basel, Switzerland) according to the manufacturer's instructions. RNA integrity was verified by agarose-gel electrophoresis and RNA was quantified by UV spectrophotometry. Reverse transcription of equal amounts of RNA was performed using ThermoScript^{TM} RT-PCR system (Invitrogen, Carlsbad, CA) and cDNA was analyzed by quantitative PCR (Light-cycler, Roche) for the ES cell-specific genes Nanog, Oct-4, and Sox2, and the metabolic housekeeping gene glyceraldehyde-3-phosphate dehydrogenase (GAPDH). Primers for GAPDH were 5′-ATTCAACGGCAC AGTCAAGG-3′ and 5′-ACCTACGT-CCCTACTACAAG-3′ (472 bp amplicon); primers for Oct-4 were 5′-CTGAGGGCCAGGC-AGGAGCACGAG-3′, and 5′-GACATCCCTCCCGAA GCCCGTGAA-3′ (484 bp amplicon); primers for Nanog (Ying et al., 2003) were 5′-ATGAAGTGCAAGCGGTGG-CAGAAA-3′ and 5′-CCTGG-TGGAGTCACAGAGTAG TTC-3′ (464 bp amplicon); and primers for Sox2 were 5′-ATGGACAGCTACGCGC-ACA-3′ and 5′-CGAGCCGTT-CATGTAGGTCTG-3′ (192 bp amplicon).

PCR reactions were carried out in glass capillary tubes in a 20 μL volume containing 1× LightCycler FastStart DNA Master Plus SYBR green, 1.5 mM $MgCl_2$, 0.2 μM of each primer for Oct-4 and 0.4 μM of each primer for Nanog and GAPDH, and 2 μL of template resulting from the reverse transcription reaction. Forty cycles were performed in a LightCycler real time PCR (Roche), each consisting of 10 s denaturation at 95°C, 5 s primer annealing at 60°C (GAPDH), 62°C (Oct-4), 57°C (Nanog) or 65°C (Sox2), and 20 s elongation at 72°C. The specificity of the reactions was confirmed using melting curve and gel electrophoresis analysis to confirm the presence of a single band. Control assays containing no templates were also performed. Results were analyzed for statistical significance using a t-test.

Microscopy

Cell growth on control plates and on Cytodex-3 was checked under an inverted microscope every day.

Samples of microcarriers were taken on days 4 and 8 and incubated at 37°C for 45 min with MTT (3(4,5-dimethylthiazol-2-yl)-2,5-diphenyltetrazolium bromide, Sigma) to assess metabolic activity. MTT, a soluble yellow salt, is converted by the mitochondria into an insoluble purple formazan salt.

Cells were fixed in 1% (v/v) paraformaldehyde in PBS and immunofluorescence was performed using standard techniques. Primary antibody against β-gal (ABCAM) was used at the dilution of 1:1,000 and secondary antibody Alexa Fluo-488 anti-rabbit at the dilution of 1:400. Nuclei were stained with 4′, 6-diamino-2-phenylindole dilactate (Dapi, Sigma). Cells were visualized under a fluorescence microscope and images were acquired with digital camera Leica DC350F and Adobe Photoshop software.

Kinetic Analysis

A simple first order kinetic model for cell expansion and death was used to interpret the experimental results obtained in stirred microcarrier cultures and control plates. The balance for viable cells (X_v) can be written as $\frac{dX_v}{dt} = \mu \cdot X_v - k_d \cdot X_v = \mu_{app} \cdot X_v$, where μ and k_d are the growth and death rates, respectively, and μ_{app} is the apparent growth rate. The calculated values were based on the initial and final cell densities.

The maximum growth rates (μ_{max}) were also estimated, using the same model applied to the slope of the curves during the exponential phase.

Results

Effect of Inoculum on Cell Expansion and Metabolism

The effect of inoculum on the growth of the S25 cells was determined by performing experiments in 24-well plates and in spinner flasks. Cells were seeded at three different concentrations: 1×10^4, 5×10^4, and 1×10^5 cells/mL and 50% of medium was changed every day starting on day 2. Cytodex-3 at 3 mg/mL was used for stirred microcarrier cultures. Viable cell densities, in terms of cells per mL, and viabilities obtained in two independent runs are represented in Figure 1. Table II compares the initial and final cell densities in terms of cells per mL and cells per cm^2, as well as the fold increase achieved by the S25 cells expanded in stirred microcarrier cultures and control plates. Cells grown in spinner flasks consistently showed high viabilities (above 90%), while in the control plates an increase in cell death was observed (at some time points viabilities decreased as far as 50%).

Independent of the initial inocula, the cells after seeding exhibit a growth curve consisting of a death or lag phase followed by an exponential phase leading to the maximum cell concentration of $2.5–3.9 \times 10^6$ cells/mL or $1.0–1.5 \times 10^6$ cells/mL, for stirred microcarrier cultures and control plates, respectively. For the inocula of 1×10^4, 5×10^4, and 1×10^5 cells/mL fold increases of, respectively, 249 ± 199, 67 ± 24, and 39 ± 9 were obtained for stirred microcarrier cultures,

DOI 10.1002/bit

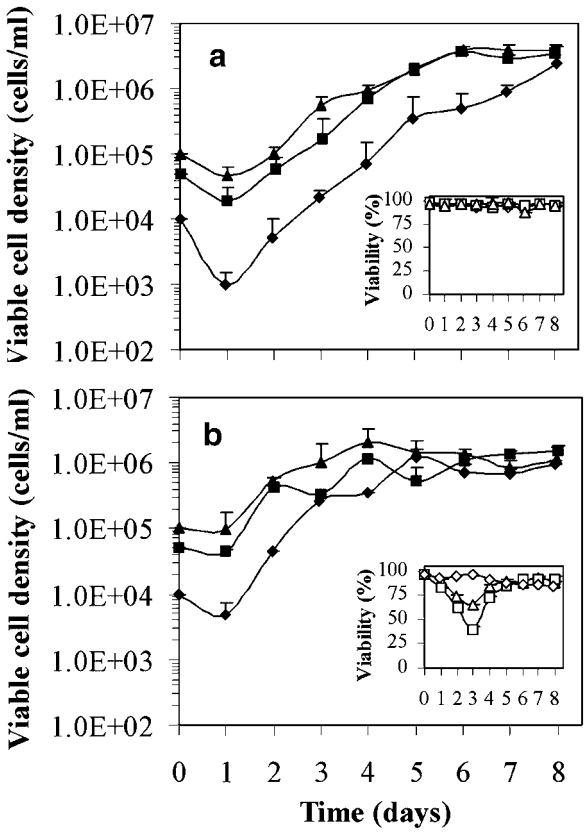

Figure 1. Effect of inoculum on the viable cell density for the S25 cells grown in: (**a**) stirred microcarriers cultures and (**b**) control plates. Cells were plated at 1×10^4 (◆, ◇), 5×10^4 (■, □), and 1×10^5 (▲, △) cells/mL in 80 or 1 mL of GMEM, for the stirred and control cultures, respectively. For stirred cultures, 3 mg of Cytodex-3 per mL were used. Media (50%) was changed every day, starting on day 2.

while significantly lower fold increases of, respectively, 99 ± 7, 31 ± 5, and 11 ± 3 were obtained for control plates.

The death or lag phase, which occurs for the first 24 h and is translated into a decrease in cell number, results from the adaptation of the cells to the culture system. This decrease is more pronounced in the stirred cultures, possibly due to poor microcarrier colonization and agitation of unattached cells, which may constitute a source of shear stress to cells.

The exponential phase continues for an extended time period for the stirred cultures (5–6 days vs. 3–4 days) and is translated into higher final cell densities in terms of cells per mL ($2.5–3.9 \times 10^6$ vs. $1.0–1.5 \times 10^6$ cells/mL), probably due to the greater available surface area as compared to control plates, which is supported by the comparison of the final cell densities in terms of cells per cm^2 that show slightly higher final cell densities for the control plates. The maximum growth rates can be estimated from the slope of the curves during this phase (Table III). Despite the differences in the inocula, the maximum growth rate is very similar for the spinners (approximately 0.050 h^{-1}). As for the plates, the exponential phase is shorter and more inconsistent, leading to lower overall growth rates (Table III). Nevertheless, the calculated maximum growth rate values are comparable with those obtained for the spinner flasks (0.048 ± 0.007 h^{-1}). In general, the obtained growth rate data, although slightly higher, are in accordance with reported data for other mouse ES cell lines (Fok and Zandstra, 2005; Oh et al., 2005; Viswanathan et al., 2003).

In the spinner cultures and for the lower inocula, the plateau stage was achieved only at the end of the experiment (day 8) and the variability throughout the experiments was higher. For the other two inocula, the cell growth was very similar and the cultures reached the maximum cell density by day 6.

To monitor cell metabolism, glucose consumption was determined. The results suggest that medium replacement allowed the supply of the nutrients and the removal of waste products inhibiting cell growth, leading to the maintenance of the cultures in steady state for several days. Figure 2 illustrates the specific glucose consumption rate and the LDH release rate. Throughout the experiments, glucose was not completely depleted from the medium (glucose concentration in the medium above 10 mM), staying within the accepted physiological range (Ozturk et al., 1997). This suggests that glucose is not a limiting factor in these cultures. LDH activity is normally used to characterize the viability status of the culture (Koller et al., 1995). In this case, LDH levels are kept low (below 21 U/L), which is in accordance with the low cell death observed in the stirred cultures.

The specific rate of glucose consumption was higher during the first 3 days of culture; afterwards, the rate

Table III. Apparent (μ_{app}) and maximum (μ_{max}) growth rates calculated using a first order kinetic model, for the S25 cells grown in stirred microcarrier cultures and control plates.

	Stirred microcarrier cultures		Control plates	
Initial cell density (cells/mL)	μ_{app} (h^{-1})	μ_{max} (h^{-1})	μ_{app} (h^{-1})	μ_{max} (h^{-1})
1×10^4	0.045 ± 0.001	0.055 ± 0.010	0.028 ± 0.002	0.055 ± 0.002
5×10^4	0.034 ± 0.007	0.051 ± 0.007	0.017 ± 0.002	0.042 ± 0.002
	0.034 ± 0.002*	0.051 ± 0.004*		
1×10^5	0.028 ± 0.002	0.045 ± 0.009	0.010 ± 0.003	0.048 ± 0.013
Average	—	0.050 ± 0.004	—	0.048 ± 0.007

For stirred cultures, 3 mg of Cytodex-3 per mL were used for the different inocula. The values denoted with an asterisk were obtained when using 0.5 mg of Cytodex-3 per mL.

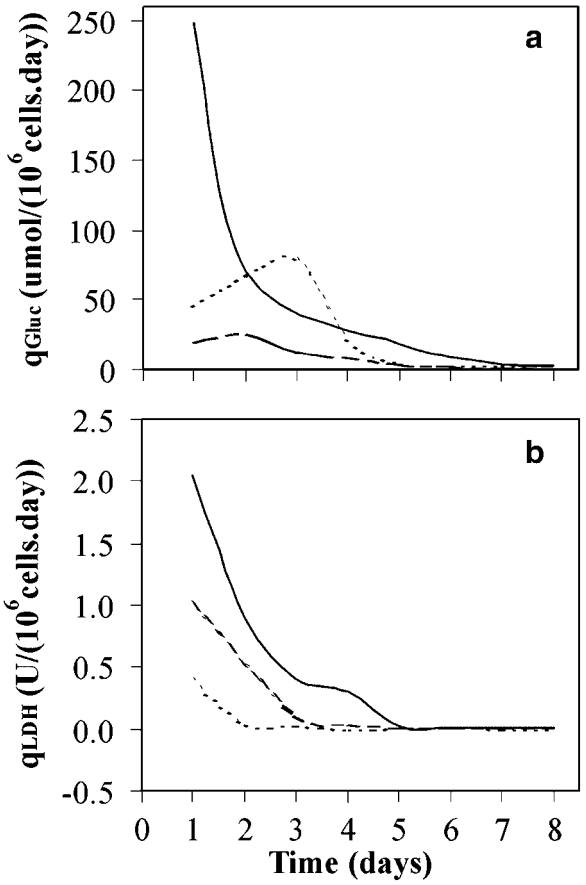

Figure 2. Effect of inoculum on the: (**a**) specific glucose consumption and (**b**) LDH release rates, for the S25 cells grown in stirred microcarriers cultures. Cells were plated at 1×10^4 (—), 5×10^4 (----), and 1×10^5 (– –) cells/mL in 80 mL of GMEM in the presence of 3 mg of Cytodex-3 per mL. Media (50%) was changed every day, starting on day 2.

decreased and by day 5, it became constant throughout the remaining culture period (approximately 5.3, 2.5, and 2.3 μmol/(10^6 cells · day), respectively, for the inocula of 1×10^4, 5×10^4, and 1×10^5 cells/mL). This may suggest that there is initial higher metabolic stress followed by adaptation and consistent metabolic behavior of the cells in the spinner flasks. The values are in accordance with other reported data (Nyberg et al., 1994; Santos et al., 2005).

These data show that, for given culture conditions, an inoculum of 5×10^4 cells/mL is sufficient to achieve the maximum cell density (approximately 3.4×10^6 cells/mL) in the shortest time period and with lower SDs. Therefore, this initial cell density was used in all subsequent experiments.

Effect of Microcarrier Concentration on Cell Expansion and Metabolism

The final cell concentration that can be achieved in a microcarrier culture depends not only on the adequate culture conditions but also on the available surface area for cell growth. Therefore, the effect of Cytodex-3 concentration was analyzed. Recommended concentrations of Cytodex-3 range between 0.5 and 5 mg/mL of final volume and therefore, the results shown in the previous section were obtained using the intermediate Cytodex-3 concentration of 3 mg/mL. Microscopic observation of the cultures showed the presence of significant amounts of empty beads, even at the end of the experiments when cells reached the plateau stage, and a substantial daily decrease in metabolites and media pH was observed (Fig. 3a). This suggests that the initial cell to Cytodex-3 ratio was far from optimal. For this reason, we next tested the lower microcarrier concentration of 0.5 mg/mL, obtaining the growth kinetics data represented in Figure 3.

No significant differences between viable cell densities were observed (maximum cell density of $3.4–4.0 \times 10^6$ cells/mL), leading to identical apparent and maximum growth rates (Tables II and III). Nevertheless, microscopic observation showed that at the lowest Cytodex-3 concentration, more than 95% of the beads were populated by cells at the end of the experiment (Fig. 3a).

Glucose consumption was similar for both experiments but LDH levels were slightly lower for the 0.5 mg/mL-Cytodex-3 cultures (data not shown), suggesting that this Cytodex-3 concentration did not decrease the available surface area to the extent that could be translated in the limitation of cell growth. Indeed, the specific LDH release rates plotted in Figure 3 show comparable results. In both tested conditions, the specific rate of glucose consumption followed the same trend, being higher during the first 3 days of culture, decreasing until day 5, and becoming constant throughout the remaining culture period (approximately 2.5 and 1.2 μmol/(10^6 cell · day), respectively for the Cytodex-3 concentration of 3 and 0.5 mg/mL).

The results show that 0.5 mg of Cytodex-3 per mL is adequate to support the expansion of the S25 cells at an inoculum of 5×10^4 cells/mL.

Effect of Culture Conditions on Gene Expression

One of the major concerns while developing scalable bioprocesses for the expansion of ES cells is the maintenance of the pluripotent state of the cells.

Immunostaining and quantitative RT-PCR (qRT-PCR) analyses of specific genes were performed to assess the efficient maintenance of the pluripotent state of S25 cells.

qRT-PCR of Oct-4 and Nanog was performed using *GAPDH* as the control gene. Oct-4 and Nanog are essential transcription factors for maintaining the pluripotent ES cell phenotype (Rodda et al., 2005). Published reports suggest that the primary function of Oct4 is to prevent trophectoderm differentiation of ICM and ES cells, whereas Nanog maintains pluripotency while preventing differentiation into primitive endoderm (Mitsui et al., 2003).

Figure 4 represents the levels of expression of these genes in the cultures grown in control plates and in the optimized

DOI 10.1002/bit

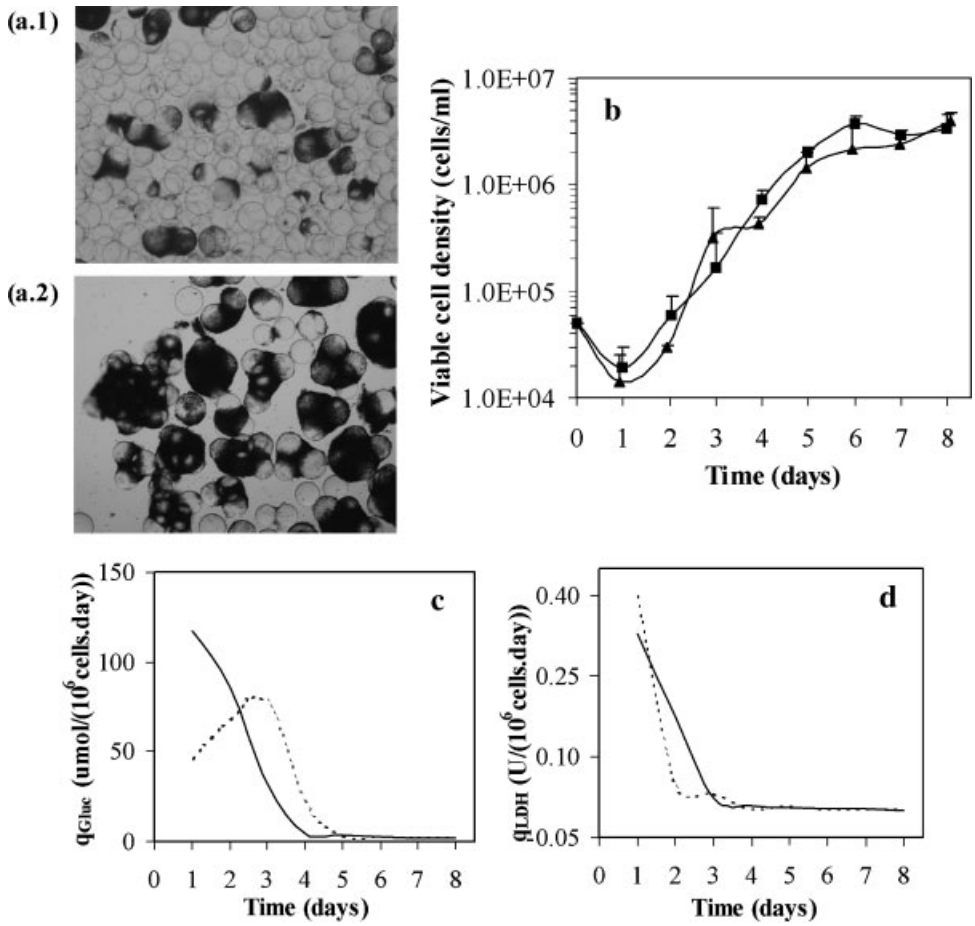

Figure 3. Effect of microcarrier concentration on the: (**a**) cell distribution on the microcarriers ((a.1) 3 mg of Cytodex-3 per mL and (a.2) 0.5 mg of Cytodex-3 per mL); (**b**) viable cell density, (**c**) specific glucose consumption rate; and (**d**) LDH release rate, of S25 cells grown in stirred microcarriers cultures. Cells were plated at 5×10^4 cells/mL in GMEM in the presence of 0.5 (▲,—) or 3 (■,----) mg of Cytodex-3 per mL. Media (50%) was changed every day, starting on day 2.

conditions in spinner flasks (0.5×10^5 cells/mL; 0.5 mg Cytodex-3/mL; 40 rpm). The results are presented as fold increases compared to day 0, normalized to the control gene data (Peirson et al., 2003; Pfaffl, 2001). In addition, qRT-PCR analysis was performed with primers for the *Sox2* gene, specific to undifferentiated ES cells and developing neuroepithelium, showing the same trend as two other pluripotency markers.

In the control plates, the levels of expression of Oct-4 decreased more than twofold by day 8 (final expression levels of 0.37 ± 0.10 relative to day 0). The Nanog RNA levels increased slightly by day 4 and then, by day 8, decreased to levels comparable to day 0 (expression levels of 1.20 ± 0.05 relative to day 0), while the levels of Sox2 remained approximately constant (expression levels of 0.81 ± 0.21 and 0.94 ± 0.09, respectively, for days 4 and 8 of culture). The marked decrease of the expression levels of the *Oct-4* gene probably reflects an increased rate of cell differentiation promoted by non-optimal culture conditions. In contrast, in the stirred system, the expression levels of all genes increased relative to day 0, suggesting an improved maintenance of the undifferentiated state in the spinner flasks. For Oct-4, average folds, relative to day 0, of 2.47 ± 0.05 and 1.28 ± 0.06 were obtained, respectively, for days 4 and 8 of culture; while for Nanog, average folds of 3.71 ± 0.56 and 3.09 ± 0.33 were obtained for the culture days 4 and 8, respectively. As for Sox2, average folds of 4.38 ± 0.14 and 3.37 ± 0.27 were obtained, respectively, for days 4 and 8 of culture.

Although the decrease in the expression levels of Nanog and Oct-4 transcription factors is associated with loss of pluripotency, their increase has different effects. Namely, increased expression of Oct-4 is similar to withdrawal of LIF, causing ES cells to differentiate preferentially into endoderm and mesoderm, while increased expression of Nanog acts in a reverse mode, preventing differentiation (Chambers et al., 2003; Niwa et al., 2000).

In this case, the increase in Oct-4 and Nanog expression in the spinner flasks was most likely the reflection of a more uniform population of pluripotent cells. The initial cell cultures used for inoculating the spinner flasks and the control plates were obtained from cell expansion in regular

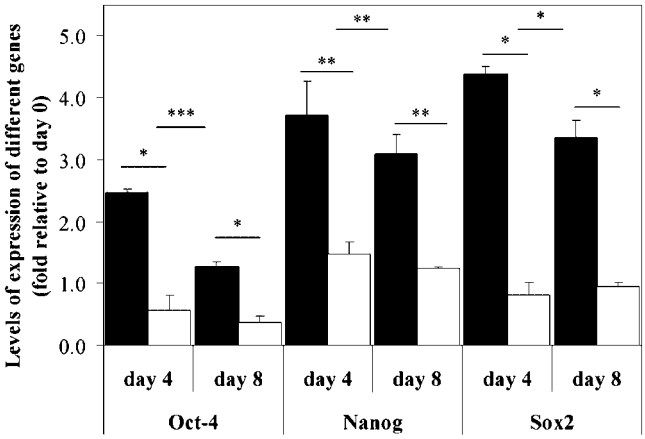

Figure 4. Effect of the culture system on the S25 ES cells expression of the pluripotency markers Oct-4, Nanog, and Sox2. Cells were plated at 5×10^4 cells/mL in GMEM on gelatin-coated plates (control plates, white bars) or, alternatively, in spinner flasks (stirred microcarrier cultures, black bars) in the presence of 0.5 mg Cytodex-3 per mL. Media (50%) were changed every day, starting on day 2. Samples that yielded statistically significant results ($^*P < 0.01$, $^{**}P < 0.05$, and $^{***}P < 0.1$ in a *t*-test) are denoted with asterisks.

petri dishes. In this system, the overgrown clusters of ES cells frequently contain a variable extent of differentiating cells on their borders, easily detectable under light microscope. In comparison to ES cells, these cells typically have higher cytoplasm-to-nucleus ratio and consequently, greater surface area. The culture conditions of the stirred system, namely the surface characteristics, favor the growth of smaller and more compact undifferentiated cells, and may reduce the probability of differentiated cells to adhere. Furthermore, the decrease in nutrients, metabolites, and gaseous gradients due to the agitation, leads to more homogeneous culture conditions, which promotes the survival and proliferation of a more uniform cell population. Therefore, the observed increase in all three pluripotency marker expression levels are indicative of more adequate culture conditions for the maintenance of these cells in an undifferentiated state.

Microscopic observation of the cell morphology and immunostaining for Sox2 expressing beta Gal transgene (Fig. 5) also confirmed the maintenance of the pluripotent state of the S25 cells grown in the spinner flasks in the optimized conditions.

Cell metabolic activity (MTT staining) was also confirmed on days 4 and 8 (Fig. 5).

Pluripotency of the cells was furthermore confirmed by measuring their differentiation potential through EBs formation. For this purpose, cells expanded in control plates and in the spinner flasks were plated on bacterial-grade petri dishes at previously optimized conditions (Abranches et al., 2006, manuscript under revision) and readily formed floating cell aggregates. After 8 days in differentiation-inducing conditions, the EBs were analyzed by PCR confirming the decrease in the expression levels of the undifferentiated markers Oct4 and Nanog, and an increase in the expression of markers from the three germ layers (not shown). In addition, dissociation of these aggregates upon 8 days in culture yielded $TujI^+$ neural precursors (not shown) indicating that the cells maintained their neural differentiation potential.

Discussion and Conclusions

Currently, the need for large numbers of stem cells for research and therapeutic applications is evident. Therefore, the growth of these cells constitutes an increasingly important bioprocess, with its feasible scale-up being a crucial aspect. Static cultures present several drawbacks (e.g., concentration gradients, difficult monitoring and control) that can be obviated using suspension culture systems such as stirred bioreactors.

The use of stirred bioreactors facilitates the expansion of cells under controlled conditions and the three-dimension microcarrier system offers advantages in terms of cell yield as compared to conventional cultures in plates. Due to their characteristics and wide use, stirred culture systems appear as promising candidates for the expansion of stem cells. For instance, several reports have been published using this system to expand bone marrow mononuclear cells (Zandstra et al., 1994), human natural killer cells (Pierson et al., 1996), hematopoietic progenitors (Collins et al., 1998a,b), neural stem cells (Sen et al., 2002b), mammary epithelial stem cells (Youn et al., 2005), primary brain astrocytes (Santos et al., 2005), and EBs (Gerecht-Nir et al., 2004; Wartenberg et al., 2001). For the expansion of ES cells, so far, a single report has been published using a stirred system (Fok and Zandstra, 2005); therefore, research should be pursued in order to achieve a better understanding of the optimum culture conditions. Recently, the use of perfusion bioreactors has also been reported for the expansion of mouse ES cells on Petriperm (Oh et al., 2005) and for the expansion of human ES cells on feeder cells (Fong et al., 2004).

As ES cells are usually expanded as anchorage-dependent cells, a support is required and microcarriers appear as a possible solution. Therefore, Cytodex-3 microcarriers were used and the effect of several culture parameters was analyzed. Improved cell growth was obtained using an inoculum of 5×10^4 cells per mL, 0.5 mg of Cytodex-3 per mL, and an agitation rate of 40 rpm.

The comparison of the maximum proliferation rates in static and suspension cultures can be used to evaluate the effect of shear stress caused by the impeller rotation. The results show that the maximum growth rates were similar, indicating that shear stress was not affecting cell growth in the spinner flasks. This was further confirmed by estimating the maximum shear stress (ι_{max}), assuming that ι_{max} was the result of flow through Kolmogorov eddies (Cherry and Kwon, 1990; Sen et al., 2002a; Youn et al., 2005). In suspension cultures, agitation is translated into the

DOI 10.1002/bit

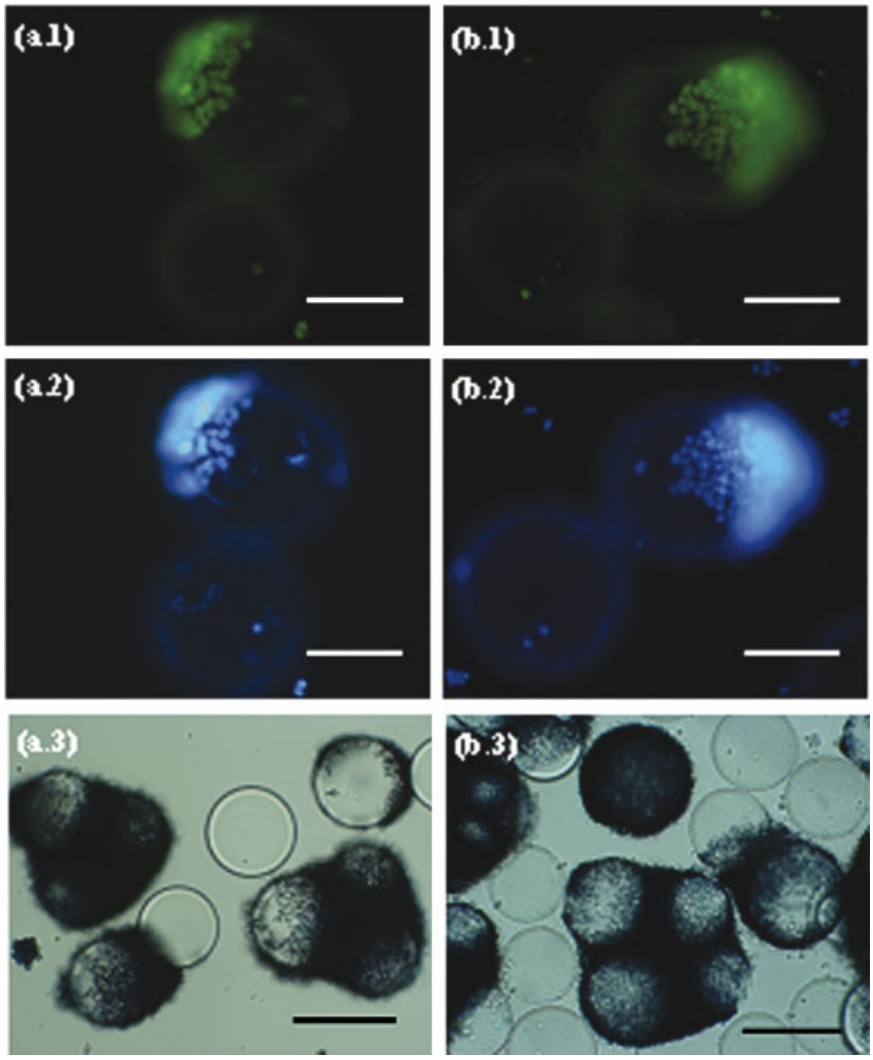

Figure 5. S25 cells grown in stirred microcarriers cultures for: (**a**) 4 days; and (**b**) 8 days. Immunocytochemistry with antibody against β-gal (a.1 and b.1, green) and nuclei labeled with Dapi (a.2 and b.2, blue). MTT staining (a.3 and b.3) to assess metabolic activity. Cells were plated at 5×10^4 cells/mL in 80 mL of GMEM in the presence of 0.5 mg Cytodex-3 per mL. Media (50%) was changed every day, starting on day 2. Scale bars: 200 μm. [Color figure can be seen in the online version of this article, available at www.interscience.wiley.com.]

formation of turbulent eddies that dissipate energy through the disintegration into Kolmogorov eddies (Cherry and Kwon, 1990). When the size of the eddies is comparable to the size of the cell aggregates, shear forces may result in reduction of the aggregates size due to the removal of cells from their surface. Even though this event may be used to control aggregate size (Sen et al., 2001), cell viability may be compromised due to shear stress. Maximum shear stress values of 15–30 dyn/cm^2 have been reported to cause damage to cells attached to surfaces (Moreira et al., 1995). Using vessel dimensions, as well as published values of medium density and viscosity (Sen et al., 2002a), the maximum shear stress for the studied agitation rate obtained was 0.47 dyn/cm^2. As expected, the obtained value is lower than the ones reported as detrimental to cells (Moreira et al., 1995). Furthermore, the results are also lower than the ones obtained for healthy suspension cultures of mouse neural stem cells (Sen et al., 2002a) and mammary epithelial stem cells (Youn et al., 2005).

The S25 ES cell line exhibited a typical growth curve, characterized by a short death or lag phase, followed by an exponential and stationary phase. In mammalian cell cultures, as well as in microbial growth, a subsequent death phase is usually observed when media change is not able to provide nutrients and remove toxic metabolic byproducts. As a preliminary study to assess if the chosen media renewal was necessary and sufficient to sustain cell needs, batch experiments were also performed (data not shown). For this purpose, cells were grown for 8 days with no media change, both in the spinner flasks and in the control plates. Contrary to what happened in the re-feed system (50% medium changed everyday, starting on day 2), in the batch experiments, the exponential phase was followed by a marked death phase. This was translated into the overall

lower final maximum cell densities, indicating that medium renewal is required in order to maximize cell growth and in this particular case, that the chosen re-feeding system was sufficient to provide adequate culture conditions.

Because ES cells grow in clusters, even when using Cytodex-3 as a support, they will be exposed to different concentrations of media components, depending on their distribution throughout the microcarriers. Glucose levels in the bulk medium were always kept within the accepted physiological range, while LDH release indicated low cell death. Nevertheless, in future studies, other media components, such as glutamine and essential amino acids, and metabolic products, such as lactic acid and ammonia, should be analyzed in order to improve the expansion of the S25 ES cells in the stirred system. Furthermore, the analysis may indicate the need for other feeding protocols. For example, dilution-feeding protocols have been reported to increase the extent of total cell expansion in the cultures of umbilical cord blood and mobilized peripheral blood mononuclear cells, in stirred and static conditions (Collins et al., 1998b).

The observation of the culture throughout time also showed the formation of colonized microcarrier aggregates, particularly after 4–5 days in culture. Although this did not seem detrimental to cells (viabilities remained high and LDH levels low), such aggregates are not desirable for reproducible bioprocesses, as they increase culture variability. A possible way to control aggregation of the microcarriers is to increase the agitation rate, and therefore, this parameter should be tested in future studies.

While testing new culture systems, cell pluripotency maintenance is essential. Morphological and biochemical monitoring of the cells grown on the microcarriers indicates that the optimized conditions are able to sustain ES cells self-renewal.

In conclusion, the growth of the S25 ES cells using the non-stationary microcarrier system is translated into high fold increases of highly purified cell populations of undifferentiated cells, with the results demonstrating the vast potential of this system for the efficient, reproducible, and cost-effective expansion of ES cells. As this mouse ES cell line has been shown to have similar proliferation rate to other feeder-independent mouse ES cell lines in self-renewal conditions (Fok and Zandstra, 2005; Oh et al., 2005; Viswanathan et al., 2003), we believe that the obtained results may be fully applicable to other feeder-independent mouse ES cell lines. Nevertheless, more research is required to better define optimal conditions for ES cell expansion and fully exploit their potential for human therapy. From the clinical point of view, mouse ES cells cannot be used for therapeutic applications, but in theory, human ES cells should behave in a similar way. Current research indicates that human ES cells are also pluripotent and exhibit similar expression of pluripotency markers, such as Oct-4, Nanog, and Sox2 (Carpenter and Bhatia, 2004; Ginis et al., 2004; Sato et al., 2003). Several differentiation protocols developed for mouse ES cell lines were successfully applied for human ES differentiation (Conti et al., 2005; Ueno et al., 2006). However, some differences have also been reported. From an engineering point of view, the knowledge gained using the mouse model will provide background and experience to expand human ES cells in bioreactors; this system may be used to study the influence of different parameters on the growth of human ES cells, such as medium composition (including the influence of different growth factors), medium renewal strategy, as well as agitation and aeration.

This work was funded by Fundação para a Ciência e a Tecnologia, Portugal (grant POCTI/BIO/46695/2002 to J.M.S.C.). E.A. was supported by a PhD fellowship from Fundação para a Ciência e a Tecnologia, Portugal (BD/6185/2001).

References

Abranches E, Bekman E, Henrique D, Cabral JMS. 2003. Expansion and neural differentiation of embryonic stem cells in adherent and suspension cultures. Biotechnol Lett 25:725–730.

Abranches E, Henrique D, Cabral JMS. 2006. Kinetic analysis of mouse embryonic stem cell growth. Manuscript under revision.

Amersham-Biosciences. Microcarrier cell culture: Principles & methods. 18-1140-62.

Bain G, Kitchens D, Yao M, Huettner JE, Gottlieb DI. 1995. Embryonic stem cells express neuronal properties in vitro. Dev Biol 168:342–357.

Billon N, Jolicoeur C, Ying QL, Smith A, Raff M. 2002. Normal timing of oligodendrocyte development from genetically engineered, lineage-selectable mouse ES cells. J Cell Sci 115:3657–3665.

Carpenter MK, Bhatia M. 2004. Characterization of human embryonic stem cells. Handbook of Stem Cells. Washington, DC: Academic Press. p 407–411.

Chambers I, Colby D, Robertson M, Nichols J, Lee S, Tweedie S, Smith A. 2003. Functional expression cloning of nanog, a pluripotency sustaining factor in embryonic stem cells. Cell 113:643–655.

Cherry RS, Kwon K-Y. 1990. Transient shear stresses on a suspension cell in turbulence. Biotechnol Bioeng 36:563–571.

Collins PC, Miller WM, Papoutsakis ET. 1998a. Stirred culture of peripheral and cord blood hematopoietic cells offers advantages over traditional static systems for clinically relevant applications. Biotechnol Bioeng 59:534–543.

Collins PC, Nielsen LK, Patel SD, Papoutsakis ET, Miller WM. 1998b. Characterization of hematopoietic cell expansion, oxygen uptake, and glycolysis in a controlled, stirred-tank bioreactor system. Biotechnol Prog 14:466–472.

Conti L, Pollard SM, Gorba T, Reitano E, Toselli M, Biella G, Sun Y, Sanzone S, Ying Q-L, Cattaneo E, et al. 2005. Niche-independent symmetrical self-renewal of a mammalian tissue stem cell. PLoS Biology 3:e283.

Evans M, Kaufman M. 1981. Establishment in culture of pluripotential cells from mouse embryos. Nature 292:154–156.

Fok EYL, Zandstra PW. 2005. Shear-controlled single-step mouse embryonic stem cell expansion and embryoid body-based differentiation. Stem Cells 23:1333–1342.

Fong W, Tan H, Choo A, Oh S. 2004. Perfusion cultures of human embryonic stem cells. Bioprocess Biosyst Eng 27:381–387.

Fraichard A, Chassande O, Bilbaut G, Dehay C, Savatier P, Samarut J. 1995. In vitro differentiation of embryonic stem cells into glial cells and functional neurons. J Cell Sci 108:3181–3188.

Gerecht-Nir S, Cohen S, Itskovitz-Eldor J. 2004. Bioreactor cultivation enhances the efficiency of human embryoid body (hEB) formation and differentiation. Biotechnol Bioeng 86:492–502.

Ginis I, Luo Y, Miura T, Thies R, Brandenburg R, Gerecht-Nir S, Amit M, Hoke A, Carpenter M, Itskovitz-Eldor J, et al. 2004. Differences between human and mouse embryonic stem cells. Dev Biol 269:360–380.

DOI 10.1002/bit

Keller G. 1995. In vitro differentiation of embryonic stem cells. Curr Opin Cell Biol 7:862–869.

Koller M, Bradley M, Palsson B. 1995. Growth factor consumption and production in perfusion cultures of human bone marrow correlate with specific cell production. Exp Hematol 23:1275–1283.

Li M, Pevny L, Lovell-Badge R, Smith A. 1998. Generation of purified neural precursors from embryonic stem cells by lineage selection. Curr Biol 8:971–974.

Martin G. 1981. Isolation of a pluripotent cell line from early mouse embryos cultured in medium conditioned by teratocarcinoma stem cells. PNAS 78:7634–7638.

Mitsui K, Tokuzawa Y, Itoh H, Segawa K, Murakami M, Takahashi K, Maruyama M, Maeda M, Yamanaka S. 2003. The homeoprotein Nanog is required for maintenance of pluripotency in mouse epiblast and ES cells. Cell 113:631–642.

Moreira JL, Alves PM, Aunins JG, Carrondo MJT. 1995. Hydrodynamic effects on BHK cells grown as suspended natural aggregates. Biotechnol Bioeng 46:351–360.

Niwa H, Miyazaki J-i, Smith AG. 2000. Quantitative expression of Oct-3/4 defines differentiation, dedifferentiation or self-renewal of ES cells. Nat Genetics 24:372–376.

Nyberg S, Remmel R, Mann H, Peshwa M, Hu W, Cerra F. 1994. Primary hepatocytes outperform Hep G2 cells as the source of biotransformation functions in a bioartificial liver. Ann Surg 226:59–67.

Oh SKW, Fong WJ, Teo Y, Tan HL, Padmanabhan J, Chin ACP, Choo ABH. 2005. High density cultures of embryonic stem cells. Biotechnol Bioeng 91:523–533.

Ozturk SS, Thrift JC, Blackie JD, Naveh D. 1997. Real-time monitoring and control of glucose and lactate concentrations in a mammalian cell perfusion reactor. Biotechnol Bioeng 53:372–378.

Peirson SN, Butler JN, Foster RG. 2003. Experimental validation of novel and conventional approaches to quantitative real-time PCR data analysis. Nucleic Acids Res 31:e73.

Pfaffl MW. 2001. A new mathematical model for relative quantification in real-time RT-PCR. Nucleic Acids Res 29:2002–2007.

Pierson B, Europa A, Hu W, Miller J. 1996. Production of human natural killer cells for adoptive immunotherapy using a computer-controlled stirred-tank bioreactor. J Hematother 5:475–483.

Rathjen J, Haines B, Hudson K, Nesci A, Dunn S, Rathjen P. 2002. Directed differentiation of pluripotent cells to neural lineages: Homogeneous formation and differentiation of a neurectoderm population. Development 129:2649–2661.

Reuveny S. 1990. Microcarrier culture systems. In: Lubiniecki AS, editor. Large-scale mammalian cell culture technology. New York: Marcel Dekker Inc.

Rodda DJ, Chew J-L, Lim L-H, Loh Y-H, Wang B, Ng H-H, Robson P. 2005. Transcriptional regulation of Nanog by OCT4 and SOX2. J Biol Chem 280:24731–24737.

Santos SS, Fonseca LL, Monteiro MAR, Carrondo MJT, Alves PM. 2005. Culturing primary brain astrocytes under a fully controlled environment in a novel bioreactor. J Neurosci Res 79:26–32.

Sato N, Sanjuan I, Heke M, Uchida M, Naef F, Brivanlou A. 2003. Molecular signature of human embryonic stem cells and its comparison with the mouse. Dev Biol 260:404–413.

Sen A, Kallos MS, Behie LA. 2001. Effects of hydrodynamics on cultures of mammalian neural stem cell aggregates in suspension bioreactors. Ind Eng Chem Res 40:5350–5357.

Sen A, Kallos MS, Behie LA. 2002a. Expansion of mammalian neural stem cells in bioreactors: Effect of power input and medium viscosity. Dev Brain Res 134:103–113.

Sen A, Kallos MS, Behie LA. 2002b. Passaging protocols for mammalian neural stem cells in suspension bioreactors. Biotechnol Prog 18:337–345.

Smith AG. 2001. Embryo-derived Stem Cells: Of Mice and Men. Annu Rev Cell Dev Biol 17:435–462.

Ueno M, Matsumura M, Watanabe K, Nakamura T, Osakada F, Takahashi M, Kawasaki H, Kinoshita S, Sasai Y. 2006. Neural conversion of ES cells by an inductive activity on human amniotic membrane matrix. PNAS 103:9554–9559.

van Wezel A. 1967. Growth of cell strains and primary cells on microcarriers in homogeneous culture. Nature 216:64–65.

Viswanathan S, Benatar T, Mileikovsky M, Lauffenburger DA, Nagy A, Zandstra PW. 2003. Supplementation-dependent differences in the rates of embryonic stem cell self-renewal, differentiation, and apoptosis. Biotechnology and Bioengineering 84:505–517.

Wartenberg M, Donmez F, Ling FC, Acker H, Hescheler J, Sauer H. 2001. Tumor-induced angiogenesis studied in confrontation cultures of multicellular tumor spheroids and embryoid bodies grown from pluripotent embryonic stem cells. FASEB J 15:995–1005.

Ying Q-L, Nichols J, Chambers I, Smith A. 2003. BMP Induction of Id proteins suppresses differentiation and sustains embryonic stem cell self-renewal in collaboration with STAT3. Cell 115:281–292.

Youn BS, Sen A, Kallos MS, Behie LA, Girgis-Gabardo A, Kurpios N, Barcelon M, Hassell JA. 2005. Large-scale expansion of mammary epithelial stem cell aggregates in suspension bioreactors. Biotechnol Prog 21:984–993.

Zandstra P, Eaves C, Piret J. 1994. Expansion of hematopoietic progenitor cell populations in stirred suspension bioreactors of normal human bone marrow cells. Biotechnology 12:909–914.